Democratic mass matrices from five dimensions

A. Soddu* and N-K. Tran†
Department of Physics, University of Virginia, 382 McCormick Road, P.O. Box 400714, Charlottesville, Virginia 22904-4714, USA
(Received 25 August 2003; published 30 January 2004)

We reconstruct the standard model quark masses and the Cabibbo-Kobayashi-Maskawa (CKM) matrix from a five-dimensional model, with the fifth dimension compactified on an S^1/Z_2 orbifold. Fermions are localized only at the orbifold fixed points and the induced quark mass matrices are almost democratic. Two specific versions of our model with 15 and 24 parameters are presented, and for both versions we can reproduce the quark mass spectrum and CKM matrix correctly to the level they are observed in current experiments.

DOI: 10.1103/PhysRevD.69.015010 PACS number(s): 11.25.Mj, 12.15.Ff

I. INTRODUCTION

The standard model (SM) has been the most satisfactory and widely recognized theory of particle interaction. To an extent, this is an effective theory, certain parameters of which are estimated and then refined by increasing high-precision experiments. However, this also means that the dynamical origin of some of these parameters is not found within the SM. One example is the pattern of family mixing characterized by the Cabibbo-Kobayashi-Maskawa (CKM) matrix, which in turn is related to the SM fermion mass spectrum and *CP* violation. Recently, considerable attention has been directed to phenomenological models with extra dimensions since, among many other things, they can offer potential answers to puzzling questions related to the SM.

In theories with compact extra dimensions, each original field in higher-dimensional space can be effectively ''viewed'' as a tower of Kaluza-Klein (KK) states in equivalent 4D theories after compactification processes. If the SM is assumed to be the low-energy manifestation of a higher-dimensional theory, the tower's lowest state (or KK zero mode) is identified as a SM field. In Ref. [1] (see also earlier works [2,3]), by introducing a Z_2-invariant Yukawa interaction between a background scalar field and a fermion field in 5D theory, after an S^1/Z_2 compactification, one can obtain a nontrivial (i.e., localized) solution for the KK zero-mode wave function along the fifth dimension (brane scenario). From a 4D point of view, any interaction term is now associated with a coupling being the overlap integration of extra dimensional wave functions of related fields. One then can flexibly control this 4D theory effective coupling by regulating the localized wave functions along the extra dimension. This very interesting mechanism has found potential applications in many problems such as proton decay suppression [3,4], fermion mass hierarchy [5–9], *CP* violation [10,12], etc.

In this work, we discuss the problem of the quark mass spectrum and mixing angles by making extensive use of a democratic structure for the mass matrices. We find that a democratic structure for the mass matrices (DMM) is a particularly convenient choice, because it raises quite naturally in the brane picture, and it can adequately generate both the quark mass spectrum and CKM matrix to the precision determined by current experimental data. Previous works dealing with fermion mass hierarchy and *CP* violation within the split-fermion scenario [6,9–12] focus on placing fermion families on different positions in the bulk, with the possibility to make mass matrix elements, originating from couplings between geographically very distant families, approximately zero. This highly hierarchical mass matrix approach, however, requires additional techniques (see Sec. II) because naively localizing fermions in an arbitrary position along the extra dimension may contradict the S^1/Z_2 orbifold compactification being used. In the DMM approach, we can avoid this subtlety by localizing all fields only at the two fixed points of the orbifold, while we break the family symmetry by modifying the detailed shapes of their wave functions. Further, the approach turns out to be more symmetric too.

Our work is structured as follows: in Sec. II we introduce the Lagrangian to generate pure-phase mass matrices (PPMM) and DMM within a fermion localization mechanism, in Sec. III we give the description of parameter space, and in Sec. IV we present the numerical method and report the results for the mass spectrum and CKM matrix for the 24 parameter version of our model and in Sec. V for the 15 parameter version. Finally we give a brief conclusion of the work in Sec. VI.

II. FORMALISM

A. Fermion localization mechanism

We first briefly review the mechanism of fermion localization in extra dimensions [1–3]. We begin with the 5D Lagrangian for a single massless fermion interacting with a real background scalar field. The fifth dimension is compact with support $[0,L]$. The generalization to the case with different families of fermions is straightforward:

$$\mathcal{L}=\overline{\psi}(x,y)[i\gamma^{\mu}\partial_{\mu}-\gamma^{5}\partial_{y}-f\phi(x,y)]\psi(x,y) + \tfrac{1}{2}\partial^{\mu}\phi(x,y)\partial_{\mu}\phi(x,y)-\tfrac{1}{2}\partial_{y}\phi(x,y)\partial_{y}\phi(x,y) - \frac{\lambda}{4}[\phi^{2}(x,y)-V^{2}]^{2}. \quad (1)$$

*Electronic address: asoddu@hep1.phys.ntu.edu.tw
†Electronic address: nt6b@galileo.phys.virginia.edu

It is important that this Lagrangian is invariant under a Z_2 symmetry[1]

$$\phi(x,y)\to\Phi(x,y)\equiv-\phi(x,L-y), \tag{2}$$

$$\psi(x,y)\to\Psi(x,y)\equiv\gamma_5\psi(x,L-y). \tag{3}$$

To obtain the chiral zero mode for fermions as they are in the SM, it is necessary to compactify the 5D theory on an S^1/Z_2 orbifold through the imposition of the following relations on the fields,

$$\phi(x,-y)=\Phi(x,L-y)=\phi(x,2L-y), \tag{4}$$

$$\psi(x,-y)=\Psi(x,L-y)=\psi(x,2L-y), \tag{5}$$

which constrain the fermion left-handed component and the scalar wave functions to be antisymmetric, and the fermion right-handed component to be symmetric at the orbifold fixed points $y=0,L$. This in turn gives rise to a stable and nonconstant VEV solution for the background scalar field when L is sufficiently large ($L>1/\sqrt{\lambda V^2}$),

$$\langle\phi(x,y)\rangle=h(y)=V\tanh\left(\mu\frac{y}{L}\right)\tanh\left[\mu\left(1-\frac{y}{L}\right)\right]+O(e^{-\mu}), \tag{6}$$

where $\mu\equiv L\sqrt{\lambda V^2/2}$ characterizes the extent of the brane in the transverse direction, to which standard model chiral quarks are going to be confined. Clearly, the VEV kink-antikink approximation (6) holds only for $\mu>1$. After performing a chiral decomposition

$$\psi(x,y)=\psi_R(x)\xi_R(y)+\psi_L(x)\xi_L(y), \tag{7}$$

one obtains the massless (zero-mode) fermion wave functions satisfying the motion equation associated with Lagrangian (1):

$$\xi_R(y)=\frac{1}{N_R}\exp\left(-f\int_0^y h(y')dy'\right)=\frac{1}{N_R}\exp\left[F\left(\mu y+\frac{1}{\tanh\mu}\ln\frac{\cosh\mu(1-y)}{\cosh\mu y\cosh\mu}\right)\right], \tag{8}$$

$$\xi_L(y)=\frac{1}{N_L}\exp\left(f\int_0^y h(y')dy'\right)=\frac{1}{N_L}\exp\left[-F\left(\mu y+\frac{1}{\tanh\mu}\ln\frac{\cosh\mu(1-y)}{\cosh\mu y\cosh\mu}\right)\right], \tag{9}$$

where $F\equiv f\sqrt{2/\lambda}$ and $N_{L,R}$ are the normalization factors.

Now let us mention some important properties of these zero-mode solutions that are relevant to the present work. First, both solutions (8) and (9) are symmetric at the orbifold fixed points $y=0,L$, so the right component survives and the left component vanishes by contradiction with the orbifold boundary conditions (5) assuring the single-handedness of SM fermions. By inverting the sign of γ_5 in (3) one can change the chirality of the surviving fermion.

Second, the sign of the Yukawa coupling f decides the localization position of the surviving chiral zero-mode fermions along the extra dimension; if $f>0$ it is $y=0$, if $f<0$ it is $y=L$. Localizing fermions at an arbitrary location other than the two fixed points in the bulk requires additional extensions of the Lagrangian such as odd-mass terms [5] or two background scalar fields [6]. In the next section, sticking just to the minimal localization mechanism, we exhaust all possibilities of placing different $\mathrm{SU}(2)_L$ representations Q, U, and D at the two fixed points and find that, in all configurations, this is indeed sufficient to obtain the right quark mass spectrum and CKM matrix. Remarkably, this minimal localization mechanism also features a democratic structure for the quark mass matrices, because fields of identical $\mathrm{SU}(2)_L\times\mathrm{U}(1)_Y$ gauge symmetry (Q_i's, U_i's, or D_i's) are localized at the same point along the extra dimension. Small deviations from a democratic mass matrix, which is necessary in any realistic model, are realized in our approach by slightly modifying the fermions wave functions.

Third, different from other works in literature, here we make use of the exact solution for the zero-mode wave functions (8) and (9) in place of a Gaussian profile approximation.

B. Quark flavor mixing

In the spirit of SM, we now introduce three $\mathrm{SU}(2)_L$ doublets Q_i and six $\mathrm{SU}(2)_L$ singlets U_i, D_i ($i=1,2,3$) whose zero modes are identified, respectively, with the SM quark chiral components q_i, u_i, d_i after orbifold compactification. The Higgs doublet zero mode is assumed to be uniform along transverse direction [$H(x,y)=H(x)/\sqrt{L}$].

We construct a general 5D Lagrangian concerning three fermion families

$$\mathcal{L}_f=\sum_{i=1}^{3}\bar{Q}_i(x,y)i\not{D}_5Q_i(x,y)+(Q_i\leftrightarrow U_i)+(Q_i\leftrightarrow D_i)+\sum_{i,j=1}^{3}\kappa^u_{5,ij}\bar{Q}_i(x,y)i\sigma_2H^*(x,y)U_j(x,y)+\sum_{i,j=1}^{3}\kappa^d_{5,ij}\bar{Q}_i(x,y)H(x,y)D_j(x,y)+\mathrm{H.c.} \tag{10}$$

In order to obtain a PPMM in 4D effective theory, we use the following ansatz for 5D Yukawa couplings

$$\kappa^u_{5,ij}=\kappa^u_5\exp(i\theta^u_{ij}),\quad \kappa^d_{5,ij}=\kappa^d_5\exp(i\theta^d_{ij}), \tag{11}$$

with $\kappa^u_{5,ij}$ and $\kappa^d_{5,ij}$ real positive. We note in particular in the above ansatz that complex higher-dimensional Yukawa couplings have universal absolute values κ^u_5, κ^d_5 for both up and down sectors, and family symmetry is broken only in the

[1]A bare mass term of fermion is forbidden by this symmetry.

phases. The difference needed between κ_5^u and κ_5^d to eventually give rise to the up-down quark mass hierarchy can also be accommodated conveniently in the brane picture with more extra dimensions (Sec. II C). The SM quarks obtain masses via spontaneous symmetry breaking with the Higgs developing a VEV $H(x,y)\to(0,v/\sqrt{2L})^T$ (note that SM chiral fields q_{ui} and q_{di} have identical extra-dimensional wave functions because they originally come from the same doublet in higher-dimensional theory[2])

$$\int dy\,\mathcal{L}_f \to \sum_{i=1}^{3} \bar{q}_{ui}(x) i\not{\partial} q_{ui}(x) + (q_{ui}\leftrightarrow q_{di}) + (q_{ui}\leftrightarrow u_i) + (q_{ui}\leftrightarrow d_i) + \sum_{i,j=1}^{3} [\bar{q}_{ui}(x) M^u_{ij} u_j(x) + \bar{q}_{di}(x) M^d_{ij} d_j(x)] + \text{H.c.}, \tag{12}$$

where

$$M^u_{ij} = \frac{v}{\sqrt{2}} g_{Yu} \exp(i\theta^u_{ij}) \int dy\, \xi_{qi}(y)\xi_{uj}(y), \tag{13}$$

$$M^d_{ij} = \frac{v}{\sqrt{2}} g_{Yd} \exp(i\theta^d_{ij}) \int dy\, \xi_{qi}(y)\xi_{dj}(y), \tag{14}$$

with real, dimensionless effective couplings $g_{Yu}=\kappa_5^u/\sqrt{L}$ and $g_{Yd}=\kappa_5^d/\sqrt{L}$. One has to notice that a pure-phase structure for the matrices M^u and M^d arises when the left-handed zero mode of Q_i are localized at the same position along the extra dimension independently of the family index i and the same happens for the right-handed zero mode of U_i and D_i. Then as it is clear from Eqs. (13) and (14) the elements of each matrix differ only by a phase factor.

We first perform the usual transformation from gauge eigenbasis to mass eigenbasis

$$u_i = U^u_{Rij} u'_j, \quad d_i = U^d_{Rij} d'_j, \tag{15}$$

$$q^u_{Li} = U^u_{Lij} q'^u_{Lj}, \quad q^d_{Li} = U^d_{Lij} q'^d_{Lj}, \tag{16}$$

where U^u_L, U^d_L diagonalize respectively the matrices $(M^u M^{u\dagger})$, $(M^d M^{d\dagger})$:

$$\text{diag}(|m_u|^2,|m_c|^2,|m_t|^2) = U^{u\dagger}_L (M^u M^{u\dagger}) U^u_L, \tag{17}$$

$$\text{diag}(|m_d|^2,|m_s|^2,|m_b|^2) = U^{d\dagger}_L (M^d M^{d\dagger}) U^d_L, \tag{18}$$

and whose product gives the CKM matrix

$$V_{\text{CKM}} = U^{u\dagger}_L U^d_L. \tag{19}$$

The origin of *CP* violation in weak interaction is related to the phase appearing in the CKM matrix, which by virtue of above relations comes from the complexity of mass matrices (it is well known that real mass matrices do not give rise to *CP* violation). The localization mechanism in 5D theory clearly provides a direct control over the modulus of each mass matrix element, but it does nothing to their phases. That is, *a priori* M^u and M^d may possess in total 18 arbitrary phases θ^u_{ij}, θ^d_{ij}.[3] In the present work, stemming from the interest in model's simplicity, we just attribute four phases ϕ_{u1}, ϕ_{u2}, ϕ_{d1}, ϕ_{d2} to elements of M^u (say M^u_{12}, M^u_{23}) and M^d (say M^d_{12}, M^d_{23}). One can note here that Hermitian matrices $(M^u M^{u\dagger})$ and $(M^d M^{d\dagger})$ have altogether six phases, but two of them are nonphysical and can be eliminated by a simultaneous transformation involving a single diagonal phase matrix $K=\text{diag}\,(1,\exp(i\alpha),\exp(i\beta))$ [10]:

$$M^u M^{u\dagger} \to K M^u M^{u\dagger} K^\dagger, \tag{20}$$

$$M^d M^{d\dagger} \to K M^d M^{d\dagger} K^\dagger. \tag{21}$$

Now the four physical phases left in $M^u M^{u\dagger}$, $M^d M^{d\dagger}$ can be reproduced by the chosen configuration with four phases in M^u, M^d.

Let us next consider the magnitude of mass matrix elements, whose complete expressions are

$$M^u_{ij} = \frac{v}{\sqrt{2}} g_{Yu} \exp(i\theta^u_{ij}) \int dy\, \xi_{qi}(y)\xi_{uj}(y) = \frac{\exp(i\theta^u_{ij})}{N_{qi}N_{uj}} \int dy \times \exp\left[F_{qi}\left(\mu_{qi} y + \frac{1}{\tanh\mu_{qi}} \ln\frac{\cosh\mu_{qi}(1-y)}{\cosh\mu_{qi} y \cosh\mu_{qi}}\right) + F_{uj}\left(\mu_{uj} y + \frac{1}{\tanh\mu_{uj}} \ln\frac{\cosh\mu_{uj}(1-y)}{\cosh\mu_{uj} y \cosh\mu_{uj}}\right)\right], \tag{22}$$

$$M^d_{ij} = \frac{v}{\sqrt{2}} g_{Yd} \exp(i\theta^d_{ij}) \int dy\, \xi_{qi}(y)\xi_{dj}(y) = \frac{\exp(i\theta^d_{ij})}{N_{qi}N_{dj}} \int dy \times \exp\left[F_{qi}\left(\mu_{qi} y + \frac{1}{\tanh\mu_{qi}} \ln\frac{\cosh\mu_{qi}(1-y)}{\cosh\mu_{qi} y \cosh\mu_{qi}}\right) + F_{dj}\left(\mu_{dj} y + \frac{1}{\tanh\mu_{dj}} \ln\frac{\cosh\mu_{dj}(1-y)}{\cosh\mu_{dj} y \cosh\mu_{dj}}\right)\right], \tag{23}$$

[2]As long as $v/\sqrt{2}\simeq 175\,\text{GeV} < 1/L$, the Higgs zero mode is the only mode that receives nonzero VEV [14].

[3]By rotating the right-handed quark fields one can absorb 3 phases from each matrix, bringing to 12 the total number of phases.

where only θ_{12}^u, θ_{23}^u, θ_{12}^d, θ_{23}^d are the nonzero phases. Indeed, without these phases, the solution satisfying the quark mass ratios and the CKM matrix cannot be obtained [13]. Further, if these phases are small enough, the mass matrices' structure transforms from almost pure-phase $M \approx g_Y v/\sqrt{2}\{e^{i\theta_{ij}}\}$ to almost democratic $M \approx g_Y v/\sqrt{2}\{1\}$. All our numerical solutions obtained below indeed clearly reflects this democratic structure. One very important advantage of a DMM is that it has three eigenvalues of ''loose hierarchy,'' $(0,0,3g_Y v/\sqrt{2})$, and by slightly modifying the mass matrix elements from ''1'' one can reproduce the right mass spectrum and right CKM matrix. More specifically, because small differences in F's and μ's induce small modifications in the corresponding wave function profiles $\xi(y)$'s, Eqs. (22) and (23), to recover realistic quark masses we will attribute different values of F_i and μ_i to different flavors (the quartic coupling λ is kept universal). Meanwhile we preserve essential democratic structure by localizing fields from each of the three groups (doublets and up and down-type singlets) at the same point along the extra dimension regardless of family index. Choosing identical signs for F_{qi} (F_{ui}, F_{di}) for different indices i, one can fulfill this requirement.

Our approach hence is different from that of Ref. [9] where wave functions of different chiral flavors are very carefully and distinctly constructed in the bulk so that their overlaps render the correct mass spectrum. However, the associated CKM matrix found therein does not generate sufficient *CP* violation as to the level it is observed in meson rare decays (as long as the model has only one extra dimension), even when one assigns to each mass matrix element an arbitrary phase [10]. In the present work a DMM structure will be the key point to overcome this difficulty.

C. Six-dimensional model

With the model with just one extra dimension presented in the previous sections, one can fit the quark mass spectrum and CKM matrix all by twisting around the pure-phase and democratic structures of mass matrices. We in particular have employed two different 5D Yukawa couplings κ_5^u, κ_5^d $(\kappa_5^u/\kappa_5^d \sim 60$, Secs. IV and V) to generate up-down quark mass hierarchy, whose nature was not seen directly within the framework of 5D theory. In this subsection, for the purpose of completeness, we briefly mention a possible solution to this issue, which consists of adding another spatial dimension to the theory.

Beginning with six-dimensional model, we can repeat the orbifold compactification procedure for the two extra dimensions, one after the other, to secure the single chirality of zero modes. We choose to localize all doublets identically along the sixth dimension (the same holds for up-type and down-type singlets). In the result, the 5D (now effective) Yukawa coupling κ_u^5 (κ_d^5) are just the product of 6D couplings κ_u^6 (κ_d^6) and the Q-U $(Q$-$D)$ wave function overlap along the sixth dimension. So by starting with a single Yukawa coupling $(\kappa_u^6 = \kappa_d^6)$ in 6D theory, we can end up with two different 5D couplings because U and D fields have been placed differently from Q fields along the sixth dimension. Further, the phases of the mass matrices' elements could also be generated from 6D models (see details in Refs. [7], [8]). Rather, the point we would like to emphasize here is that, extra dimension theory can potentially provide the necessary ingredients to reproduce 4D effective theory of particle interaction.

III. DESCRIPTION OF THE PARAMETER SPACE

In this section we present the parameter space for the particular choice of the model considered with 24 parameters. Also if the number of parameters is large, what has to be said here is that the ''naturality'' of the parameters (generally all the values are of order one or differ by no more than one order of magnitude), we believe, is the most important factor, and the parameter space found satisfies this condition. The list of the parameters is the following:

(1) g_{Yu} and g_{Yd}.

(2) $\mu_{qi} = L\sqrt{\lambda V_{qi}^2/2}$, $\mu_{ui} = L\sqrt{\lambda V_{ui}^2/2}$, and $\mu_{di} = L\sqrt{\lambda V_{di}^2/2}$, where $i = 1,2,3$ are dimensionless quantities whose inverse is proportional to the thickness of the domain wall.

(3) $F_{qi} = \sqrt{2/\lambda} f_{qi}$, $F_{ui} = \sqrt{2/\lambda} f_{ui}$, and $F_{di} = \sqrt{2/\lambda} f_{di}$ with $i = 1,2,3$ and f's being the Yukawa couplings appearing in Eq. (1).

(4) ϕ_{u1}, ϕ_{u2}, ϕ_{d1}, and ϕ_{d2} are the phases appearing, respectively, in the up and down mass matrices.

As it can be seen from this particular choice of the parameter space, we decided to break family symmetry by choosing different values for μ_i and f_i for different indices i (together with four different phases θ_{12}^u, θ_{23}^u, θ_{12}^d, θ_{23}^d appearing in the mass matrices), and at the same time to break the left-right symmetry by different values for the left component parameters μ_q and f_q and the right component parameters μ_u, f_u, μ_d, and f_d.

IV. RESULTS FOR MASS MATRICES FROM FIVE DIMENSIONS

In this section we present the numerical results obtained for the parameter space and for the physical quantities of Table I. We consider four different cases, which correspond to all four possible ways of picking the sign of the Yukawa couplings f for the left and right components. The four different cases are the following:

(1) $f_{qi} > 0$ $f_{ui} > 0$ $f_{di} > 0$ denoted as $(+\ +\ +)$,
(2) $f_{qi} > 0$ $f_{ui} > 0$ $f_{di} < 0$ denoted as $(+\ +\ -)$,
(3) $f_{qi} > 0$ $f_{ui} < 0$ $f_{di} > 0$ denoted as $(+\ -\ +)$,
(4) $f_{qi} > 0$ $f_{ui} < 0$ $f_{di} < 0$ denoted as $(+\ -\ -)$.

The first case corresponds to the doublets and up- and down-type singlets all localized at the orbifold fixed point $y = 0$. The second case corresponds to the doublets and up-type singlets localized at $y = 0$ while the down-type singlets are localized at $y = L$. The third case corresponds to the doublets and down-type singlets localized at $y = 0$ while the up-type singlets are localized at $y = L$. And finally the fourth case corresponds to the doublets localized at $y = 0$, while both the up- and down-type singlets are localized at $y = L$.

TABLE I. Central values and uncertainties for the masses of the 6 quarks evaluated at M_Z, for the two ratios m_u/m_d and m_s/m_d, for the absolute values of the CKM matrix elements, and the *CP* parameters $\overline{\rho}$, $\overline{\eta}$.

x_i	$\langle x_i \rangle$	$\lvert x_i^{\max} - x_i^{\min} \rvert / 2$
m_u	2.33×10^{-3}	0.45×10^{-3}
m_c	0.685	0.061
m_t	181	13
m_d	4.69×10^{-3}	0.66×10^{-3}
m_s	0.0934	0.0130
m_b	3.00	0.11
m_u/m_d	0.497	0.119
m_s/m_d	19.9	3.9
$\lvert V_{ud} \rvert$	0.97485	0.00075
$\lvert V_{us} \rvert$	0.2225	0.0035
$\lvert V_{ub} \rvert$	0.00365	0.0115
$\lvert V_{cd} \rvert$	0.2225	0.0035
$\lvert V_{cs} \rvert$	0.9740	0.0008
$\lvert V_{cb} \rvert$	0.041	0.003
$\lvert V_{td} \rvert$	0.009	0.005
$\lvert V_{ts} \rvert$	0.0405	0.0035
$\lvert V_{tb} \rvert$	0.99915	0.00015
$\overline{\rho}$	0.22	0.10
$\overline{\eta}$	0.35	0.05

The other four possible cases obtained when one changes at the same time all the signs of the Yukawa couplings are just symmetrical to the four presented, with each wave function now localized at the other orbifold fixed point, and with symmetrical profile. So they do not present any new mixing pattern.

The approach we use to derive the parameter space consists of minimizing a particular function, built in such a way that its global minima correspond to the region defined by the experimental constraints. This function is defined as

$$E = \sum_{i=1}^{N} \frac{(x_i^{\text{th}} - x_i^{\min})^2}{\langle x_i \rangle^2} \theta(x_i^{\min} - x_i^{\text{th}}) + \sum_{i=1}^{N} \frac{(x_i^{\text{th}} - x_i^{\max})^2}{\langle x_i \rangle^2} \theta(x_i^{\text{th}} - x_i^{\max}), \tag{24}$$

where $\theta(x)$ is the step function, N is the number of quantities that we want to fit, x_i^{th} is the predicted value for the ith quantity, $x_i^{\min}$ and $x_i^{\max}$ fix the range for the ith quantity, and $\langle x_i \rangle$ is its average value. It is immediate to verify from Eq. (24) that when all the predicted quantities x_i^{th}'s are contained in the proper ranges, the function E takes its minimum value equal to zero. The set of parameters that correspond to a zero value for the function E is called a solution.

The minimization procedure we used is called simulated annealing [15–18], and when the function that we want to minimize depends on many parameters, this procedure seems to work more efficiently than others. In particular, the simulated annealing method is mostly used when the global minima are surrounded by a lot of local minima. In fact this minimization process can find a global minimum also after being trapped in a local minimum.

In the following we will present the characteristically important numerical results for each of the cases mentioned above. We will present graphically together with the solutions of the mass spectrum (Figs. 1–4) (masses are given in GeV and are evaluated at the M_Z scale), the CKM matrix (Figs. 5–8), and the $\overline{\rho}, \overline{\eta}$ *CP* parameters (composite Fig. 9). For each case we will also give one particular numerical complete set of its 24 defining parameters (Table II), the quark mass matrices and quark mass spectra, the CKM matrix, and the *CP* parameters. Further, just for the purpose of demonstration, we will also present a pair of numerical rotation matrices $U_L^{u\dagger}$, U_L^d, the parameter space (Fig. 10), and the plots of background scalar fields and the wave function profiles of the left and right components for the case $(+\ +\ +)$ (Fig. 11). All complex phases are measured in radians.

(1) $f_{qi} > 0\ f_{ui} > 0\ f_{di} > 0$:

$$M_{u(24)}^{(+++)} = 57.81\ \text{GeV} \begin{pmatrix} 0.9814 & 0.9811 e^{-i0.0001} & 0.9705 \\ 0.9443 & 0.9438 & 0.9268 e^{i0.0155} \\ 0.9938 & 0.9936 & 0.9870 \end{pmatrix}, \tag{25}$$

$$m_{u(24)}^{(+++)} = 0.0027\ \text{GeV}, \quad m_{c(24)}^{(+++)} = 0.677\ \text{GeV}, \quad m_{t(24)}^{(+++)} = 168.13\ \text{GeV}, \tag{26}$$

$$M_{d(24)}^{(+++)} = 0.975\ \text{GeV} \begin{pmatrix} 0.9973 & 0.9934 e^{-i0.0095} & 0.9955 \\ 0.9975 & 0.9996 & 0.9988 e^{-i0.1607} \\ 0.9880 & 0.9808 & 0.9845 \end{pmatrix}, \tag{27}$$

$$m_{d(24)}^{(+++)} = 0.0048\ \text{GeV}, \quad m_{s(24)}^{(+++)} = 0.106\ \text{GeV}, \quad m_{b(24)}^{(+++)} = 2.90\ \text{GeV}. \tag{28}$$

In Eqs. (25) and (27) the mass matrices are written in a form that better shows the almost democratic structure. In Eq. (31) we give the expression for the CKM matrix, in Eq. (33) the values for the *CP* parameters $\overline{\rho}$ and $\overline{\eta}$, and the invariant area of the unitary triangle J_{CP}:

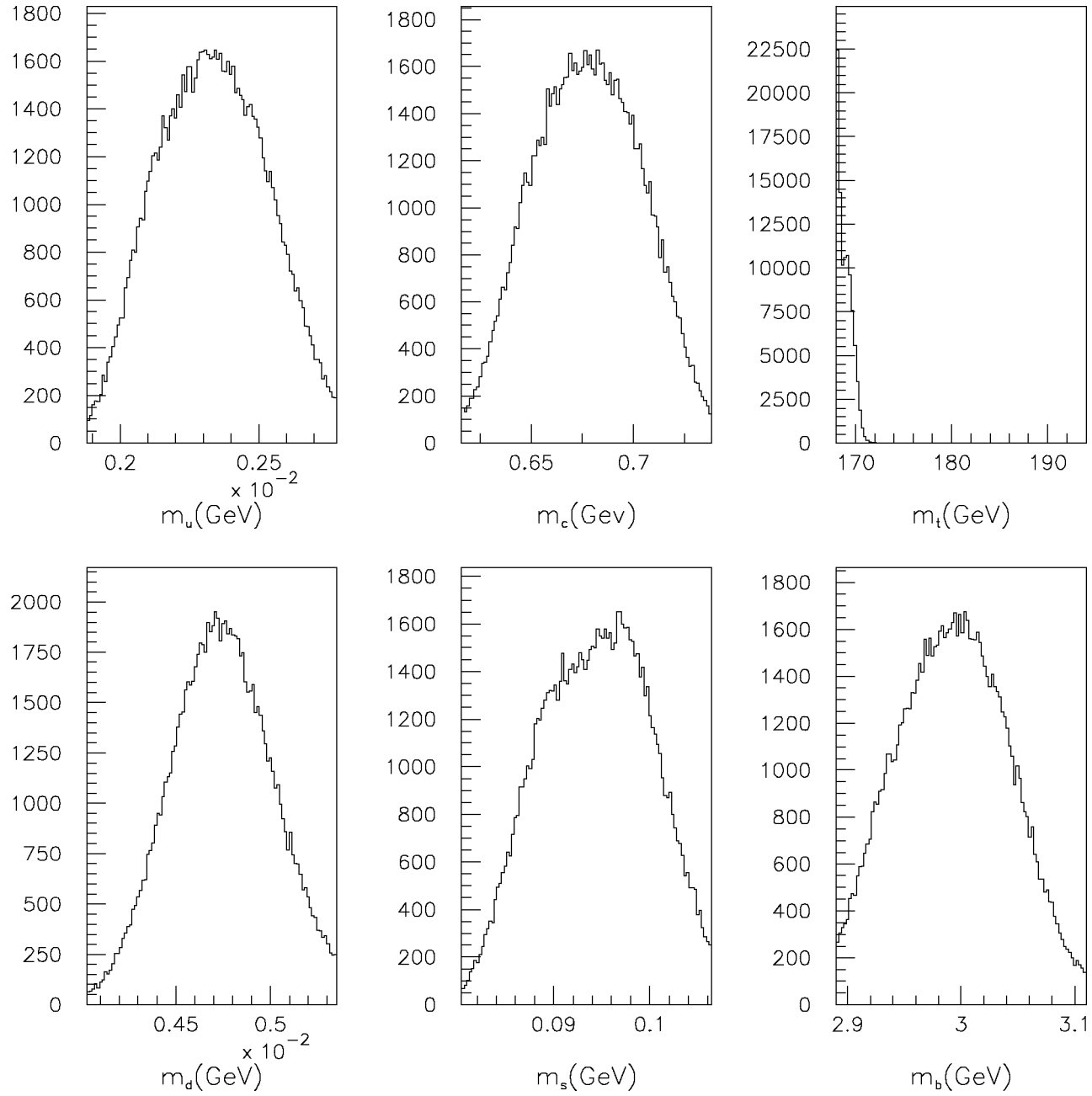

FIG. 1. Solutions for the 6 quark masses corresponding to $f_{qi}>0\, f_{ui}>0\, f_{di}>0$ for the 24 parameter space. The masses in GeV are evaluated at the M_Z scale. The range for each mass is given by the edges of the corresponding window.

$$U^{u\dagger(+++)}_{L(24)} = \begin{pmatrix} 0.7429 & -0.1027-0.1315i & -0.6361+0.1249i \\ -0.3067-0.1223i & 0.8123 & -0.4664+0.1167i \\ 0.5823 & 0.5588-0.0028i & 0.5905 \end{pmatrix}, \tag{29}$$

$$U^{d(+++)}_{L(24)} = \begin{pmatrix} -0.6924+0.0002i & -0.4298-0.0234i & 0.5783+0.0292i \\ -0.0207+0.0031i & 0.8141 & 0.5803 \\ 0.7212 & -0.3893-0.0191i & 0.5718+0.0306i \end{pmatrix}, \tag{30}$$

$$V^{(+++)}_{\mathrm{CKM}(24)} = \begin{pmatrix} -0.9706 & +0.0927i & -0.1529-0.1609i & 0.0025-0.0027i \\ -0.1408+0.1713i & 0.9741+0.0232i & 0.0274-0.0272i & \\ 0.0111+0.0019i & -0.0252-0.0272i & 0.9987+0.0334i & \end{pmatrix}, \tag{31}$$

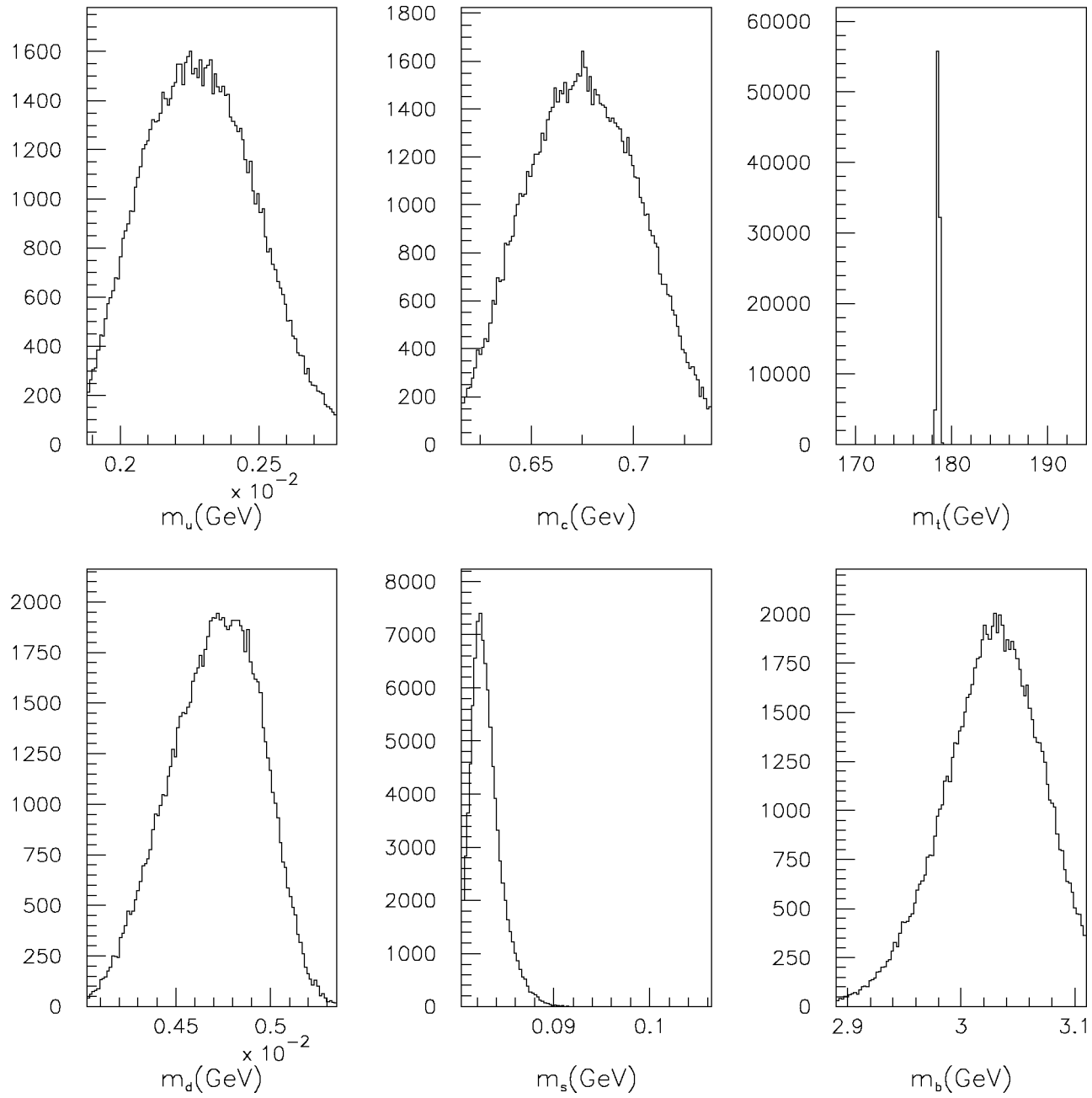

FIG. 2. Solutions for the 6 quark masses corresponding to $f_{qi}>0\, f_{ui}>0\, f_{di}<0$ for the 24 parameter case. The masses in GeV are evaluated at the M_Z scale. The range for each mass is given by the edges of the corresponding window.

$$|V_{\mathrm{CKM}(24)}^{(+++)}| = \begin{pmatrix} 0.9750 & 0.2220 & 0.0037 \\ 0.2217 & 0.9744 & 0.0386 \\ 0.0113 & 0.0371 & 0.9992 \end{pmatrix}, \tag{32}$$

$$\bar{\rho}_{(24)}^{(+++)} = 0.28, \quad \bar{\eta}_{(24)}^{(+++)} = 0.31, \quad J_{CP(24)}^{(+++)} = -2.2\times 10^{-5}, \tag{33}$$

with $\bar{\rho}$ and $\bar{\eta}$ defined as

$$\bar{\rho} = \mathrm{Re}(V_{ud}V_{ub}^{*}V_{cd}^{*}V_{cb})/|V_{cd}V_{cb}^{*}|^2, \tag{34}$$

$$\bar{\eta} = \mathrm{Im}(V_{ud}V_{ub}^{*}V_{cd}^{*}V_{cb})/|V_{cd}V_{cb}^{*}|^2, \tag{35}$$

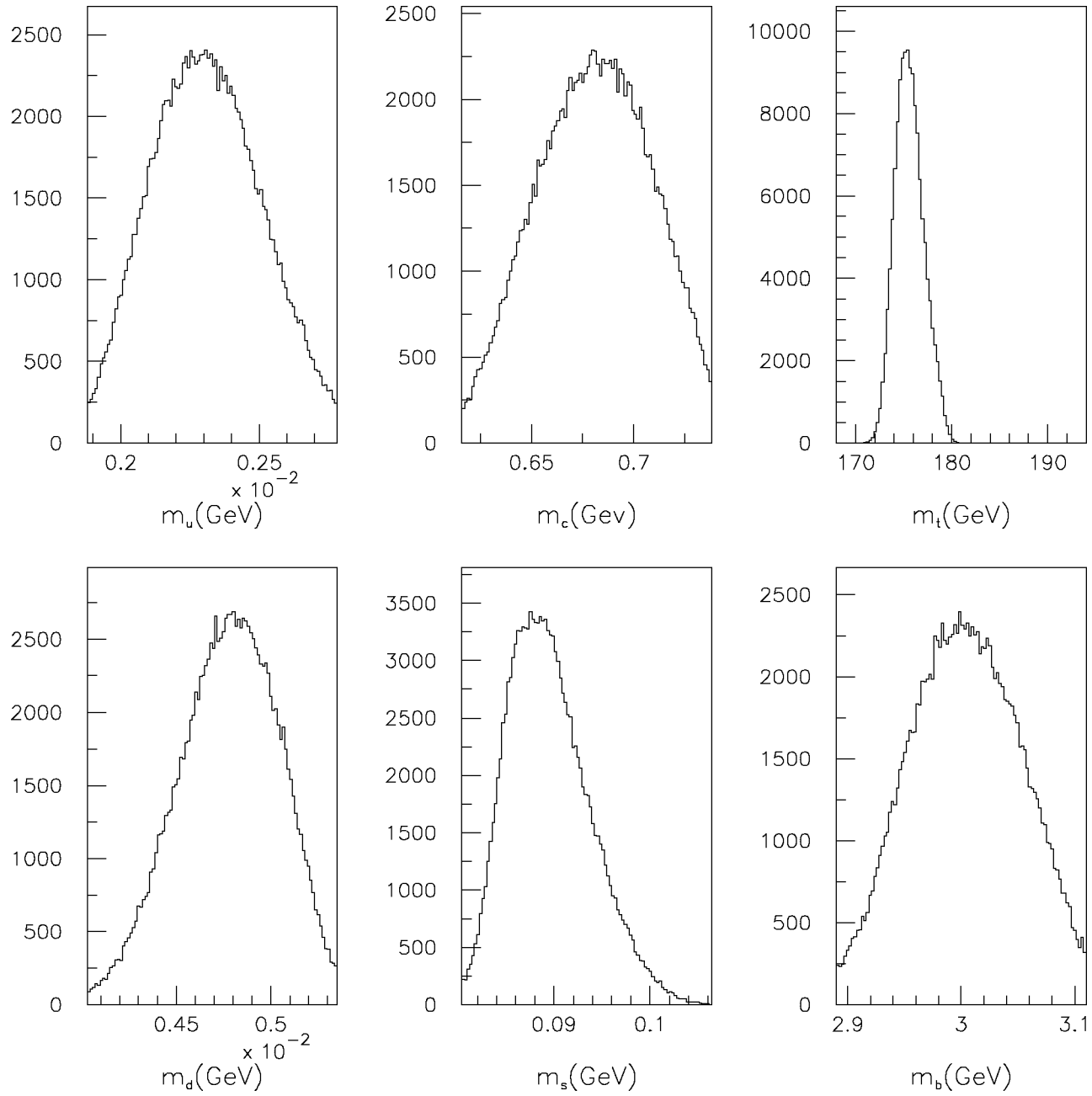

FIG. 3. Solutions for the 6 quark masses corresponding to $f_{qi}>0\, f_{ui}<0\, f_{di}>0$ for the 24 parameter case. The masses in GeV are evaluated at the M_Z scale. The range for each mass is given by the edges of the corresponding window.

and J_{CP} as

$$J_{CP}=\mathrm{Im}(V_{us}V_{ub}^{*}V_{cs}^{*}V_{cb}). \tag{36}$$

(2) $f_{qi}>0\ f_{ui}>0\ f_{di}<0$:

$$M_{u(24}^{(++-)}=59.85\ \ \mathrm{GeV}\begin{pmatrix} 0.9997 & 0.9899e^{-i0.0007} & 0.9910 \\ 0.9887 & 0.9995 & 0.9992e^{-i0.0018} \\ 0.9998 & 0.9952 & 0.9960 \end{pmatrix}, \tag{37}$$

$$m_{u(24)}^{(++-)}=0.0024\ \ \mathrm{GeV}, \quad m_{c(24)}^{(++-)}=0.722\ \ \mathrm{GeV}, \quad m_{t(24)}^{(++-)}=178.7\ \ \mathrm{GeV}, \tag{38}$$

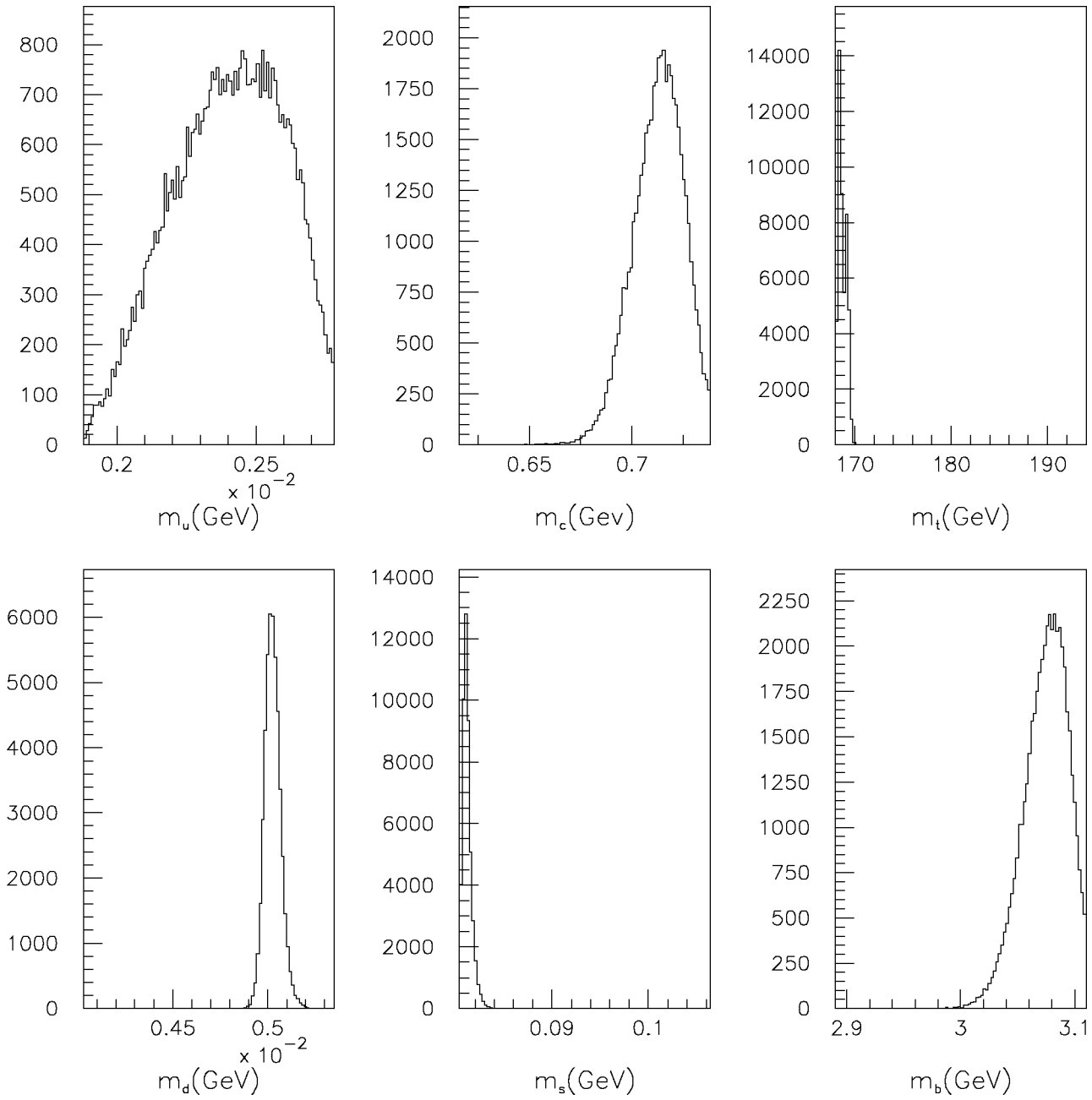

FIG. 4. Solutions for the 6 quark masses corresponding to $f_{qi}>0$, $f_{ui}<0$, $f_{di}<0$ for the 24 parameter case. The masses in GeV are evaluated at the M_Z scale. The range for each mass is given by the edges of the corresponding window.

$$M_{d(24)}^{(++-)}=1.18\ \text{GeV}\begin{pmatrix}0.8867 & 0.8337e^{i0.0122} & 0.9863\\ 0.7955 & 0.7293 & 0.9428e^{-i0.0951}\\ 0.8656 & 0.8090 & 0.9779\end{pmatrix}, \tag{39}$$

$$m_{d(24)}^{(++-)}=0.0051\ \text{GeV},\quad m_{s(24)}^{(++-)}=0.082\ \text{GeV},\quad m_{b(24)}^{(++-)}=3.1\ \text{GeV}, \tag{40}$$

$$V_{\text{CKM}(24)}^{(++-)}=\begin{pmatrix}0.9741+0.0303i & -0.1870+0.1230i & -0.0004+0.0041i\\ 0.1765+0.1373i & 0.9726+0.0479i & -0.0390-0.0177i\\ 0.0097+0.0061i & 0.0380-0.0166i & 0.9990-0.0144i\end{pmatrix}, \tag{41}$$

$$\overline{\rho}_{(24)}^{(++-)}=0.13,\quad \overline{\eta}_{(24)}^{(++-)}=0.40,\quad J_{CP(24)}^{(++-)}=-3.6\times10^{-5}. \tag{42}$$

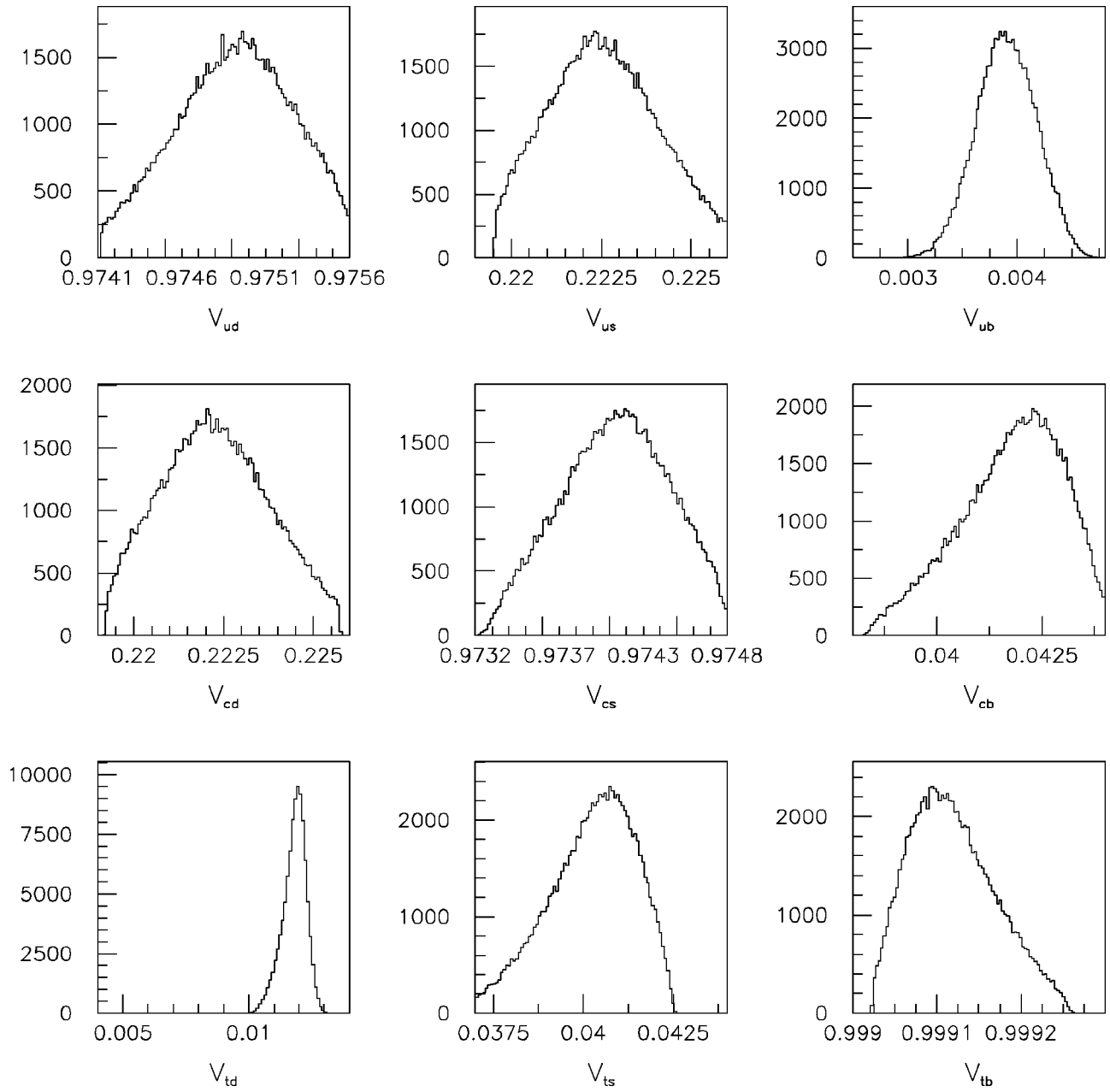

FIG. 5. Solutions for the absolute values of the CKM matrix elements corresponding to $f_{qi}>0\ f_{ui}>0\ f_{di}>0$ for the 24 parameter space. The range for each element is given by the edges of the window.

(3) $f_{qi}>0\ f_{ui}<0\ f_{di}>0$:

$$M^{(+-+)}_{u(24)} = 61.66\ \text{GeV} \begin{pmatrix} 0.9185 & 0.8840e^{-i0.0006} & 0.9032 \\ 0.9920 & 0.9785 & 0.9865e^{-i0.0000} \\ 0.9763 & 0.9557 & 0.9676 \end{pmatrix}, \tag{43}$$

$$m^{(+-+)}_{u(24)} = 0.0024\ \text{GeV}, \quad m^{(+-+)}_{c(24)} = 0.724\ \text{GeV}, \quad m^{(+-+)}_{t(24)} = 176.1\ \text{GeV}, \tag{44}$$

$$M^{(+-+)}_{d(24)} = 1.00\ \text{GeV} \begin{pmatrix} 0.9941 & 0.9357e^{i0.0870} & 0.9977 \\ 0.9851 & 0.9968 & 0.9403e^{-i0.0035} \\ 0.9967 & 0.9853 & 0.9672 \end{pmatrix}, \tag{45}$$

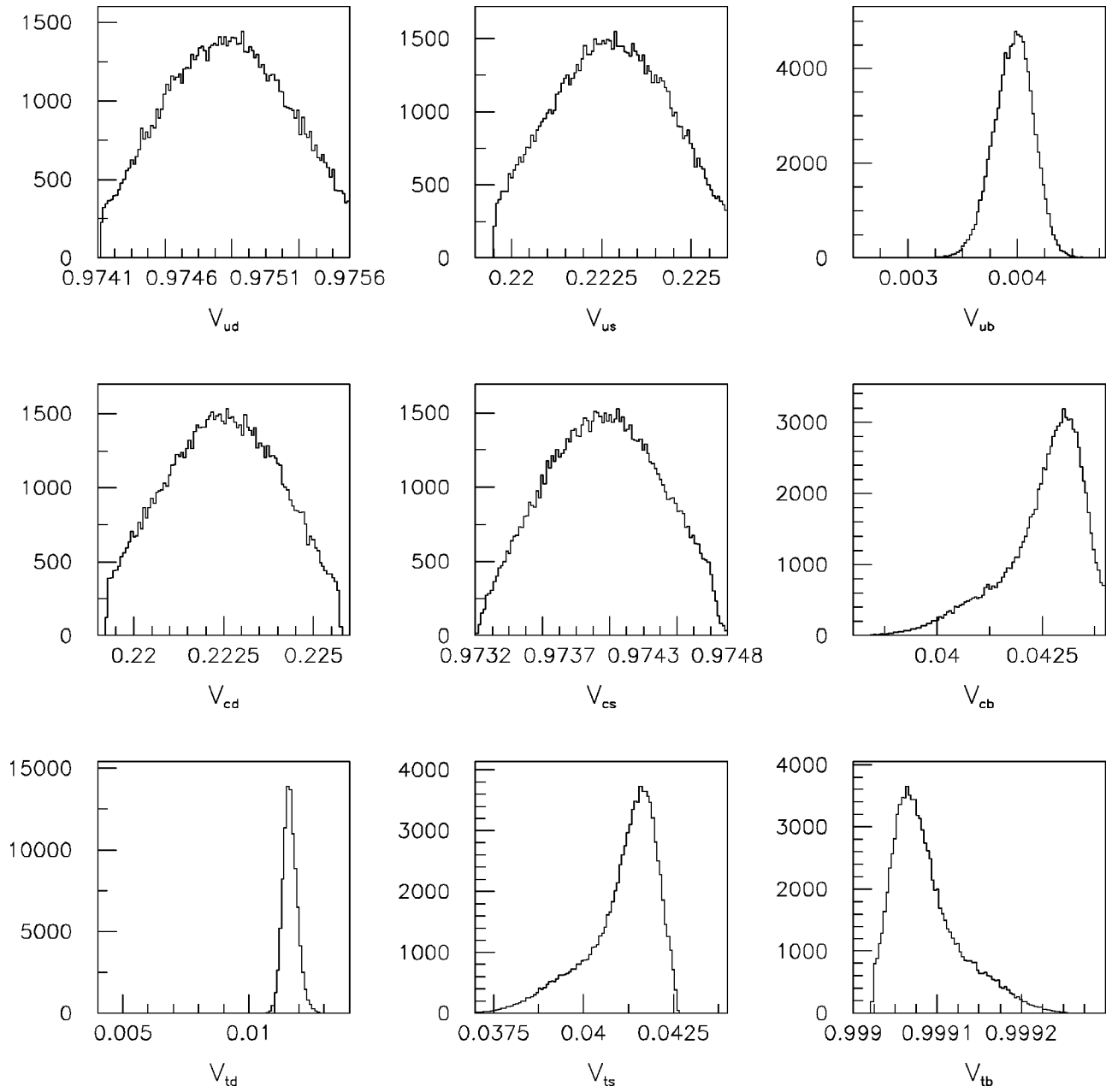

FIG. 6. Solutions for the absolute values of the CKM matrix elements corresponding to $f_{qi}>0$ $f_{ui}>0$ $f_{di}<0$ for the 24 parameter case. The range for each element is given by the edges of the window.

$$m_{d(24)}^{(+-+)}=0.0048\ \text{GeV}, \quad m_{s(24)}^{(+-+)}=0.082\ \text{GeV}, \quad m_{b(24)}^{(+-+)}=2.9\ \text{GeV}, \tag{46}$$

$$V_{\text{CKM}(24)}^{(+-+)}=\begin{pmatrix} 0.9738+0.0363i & -0.1576+0.1600i & -0.0002-0.0036i \\ 0.1437+0.1723i & 0.9727+0.0444i & 0.0370+0.0135i \\ -0.0073-0.0081i & -0.0362+0.0118i & 0.9992+0.0084i \end{pmatrix}, \tag{47}$$

$$\overline{\rho}_{(24)}^{(+-+)}=0.17, \quad \overline{\eta}_{(24)}^{(+-+)}=0.36, \quad J_{CP(24)}^{(+-+)}=-2.8\times10^{-5}. \tag{48}$$

(4) $f_{qi}>0$ $f_{ui}<0$ $f_{di}<0$:

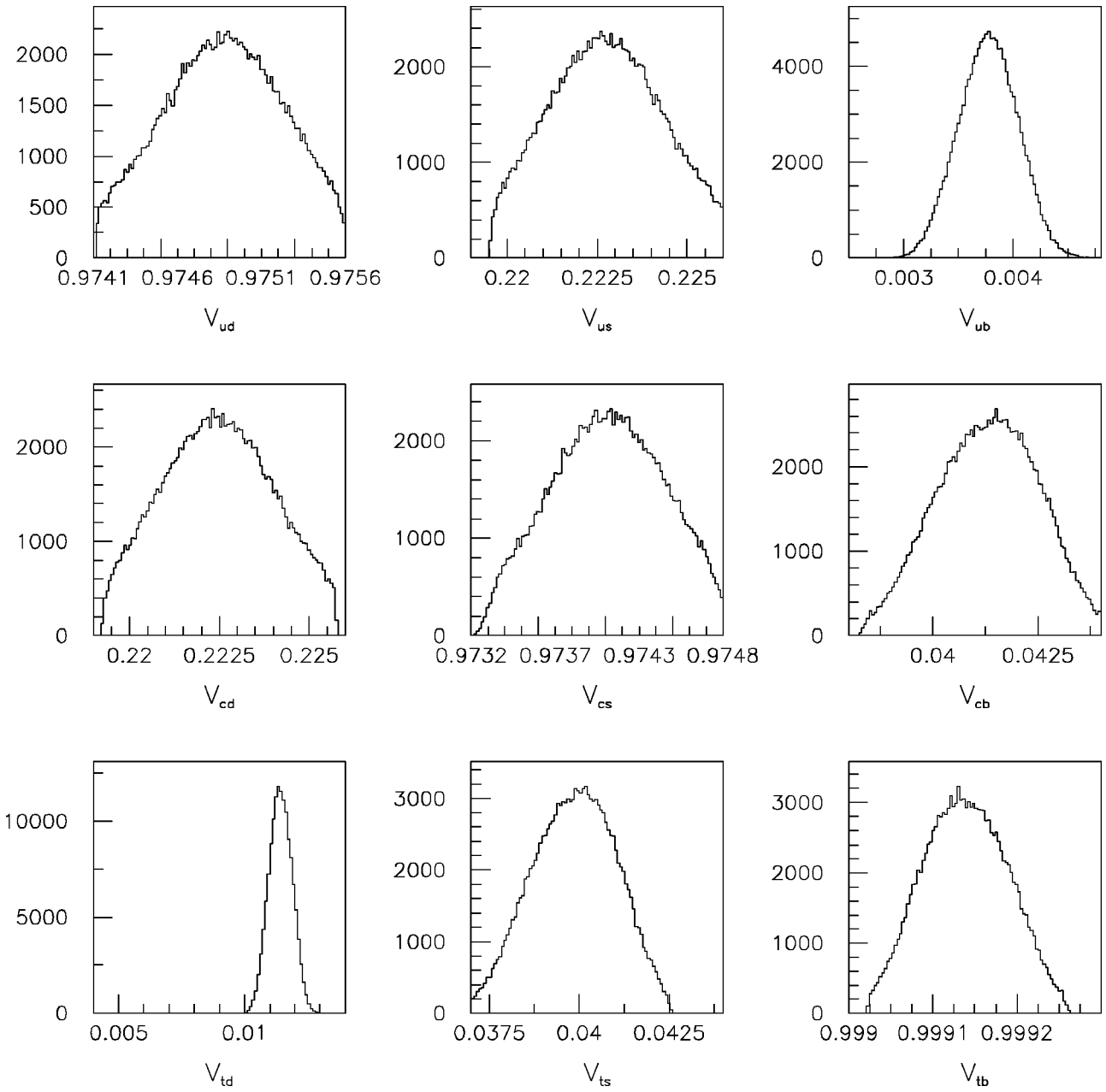

FIG. 7. Solutions for the absolute values of the CKM matrix elements corresponding to $f_{qi}>0$, $f_{ui}<0$, $f_{di}>0$ for the 24 parameter case. The range for each element is given by the edges of the window.

$$M_{u(24)}^{(+--)} = 60.83\ \text{GeV} \begin{pmatrix} 0.8427 & 0.8188e^{-i0.0053} & 0.8412 \\ 0.9893 & 0.9819 & 0.9889e^{-i0.0003} \\ 0.9447 & 0.9293 & 0.9437 \end{pmatrix}, \tag{49}$$

$$m_{u(24)}^{(+--)} = 0.0022\ \text{GeV}, \quad m_{c(24)}^{(+--)} = 0.677\ \text{GeV}, \quad m_{t(24)}^{(+--)} = 168.3\ \text{GeV}, \tag{50}$$

$$M_{d(24)}^{(+--)} = 1.25\ \text{GeV} \begin{pmatrix} 0.7298 & 0.7668e^{i0.0218} & 0.5944 \\ 0.9438 & 0.9613 & 0.8640e^{-i0.0525} \\ 0.8664 & 0.8936 & 0.7580 \end{pmatrix}, \tag{51}$$

$$m_{d(24)}^{(+--)} = 0.0050\ \text{GeV}, \quad m_{s(24)}^{(+--)} = 0.081\ \text{GeV}, \quad m_{b(24)}^{(+--)} = 3.1\ \text{GeV}, \tag{52}$$

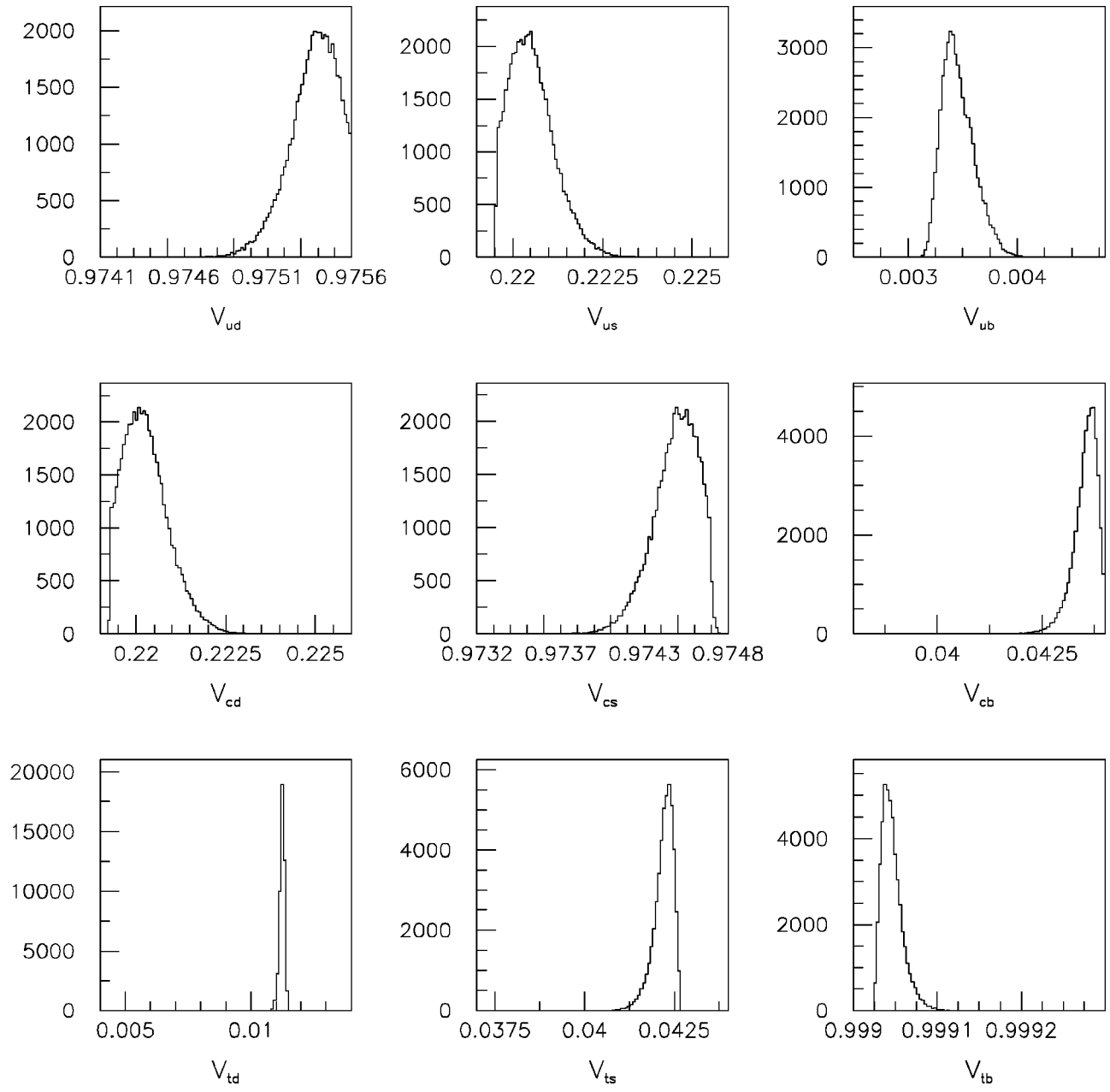

FIG. 8. Solutions for the absolute values of the CKM matrix elements corresponding to $f_{qi}>0$, $f_{ui}<0$, $f_{di}<0$ for the 24 parameter case. The range for each element is given by the edges of the window.

$$V_{\mathrm{CKM}(24)}^{(+--)}=\begin{pmatrix} 0.9755-0.0108i & 0.0848-0.2026i & -0.0025-0.0022i \\ -0.1043-0.1930i & 0.9710-0.0847i & -0.0435+0.0065i \\ -0.0007-0.0113i & 0.0426+0.0024i & 0.9990+0.0112i \end{pmatrix}, \tag{53}$$

$$\overline{\rho}_{(24)}^{(+--)}=0.13, \quad \overline{\eta}_{(24)}^{(+--)}=0.31, \quad J_{CP(24)}^{(+--)}=-2.9\times10^{-5}. \tag{54}$$

By looking at the four cases one can notice that all mass matrices have almost democratic structure with deviations from democracy for the up and down sector, which depend on the different cases. In particular, the situation with all components localized at the same orbifold fixed point (+ + +) has both mass matrices very close to a DMM. The mass matrices, except the different Yukawa prefactors, are very similar. In this case a small top mass seems to be favored (Fig. 1). For the configuration with the doublets localized at the zero orbifold fixed point and both the up and down sin-

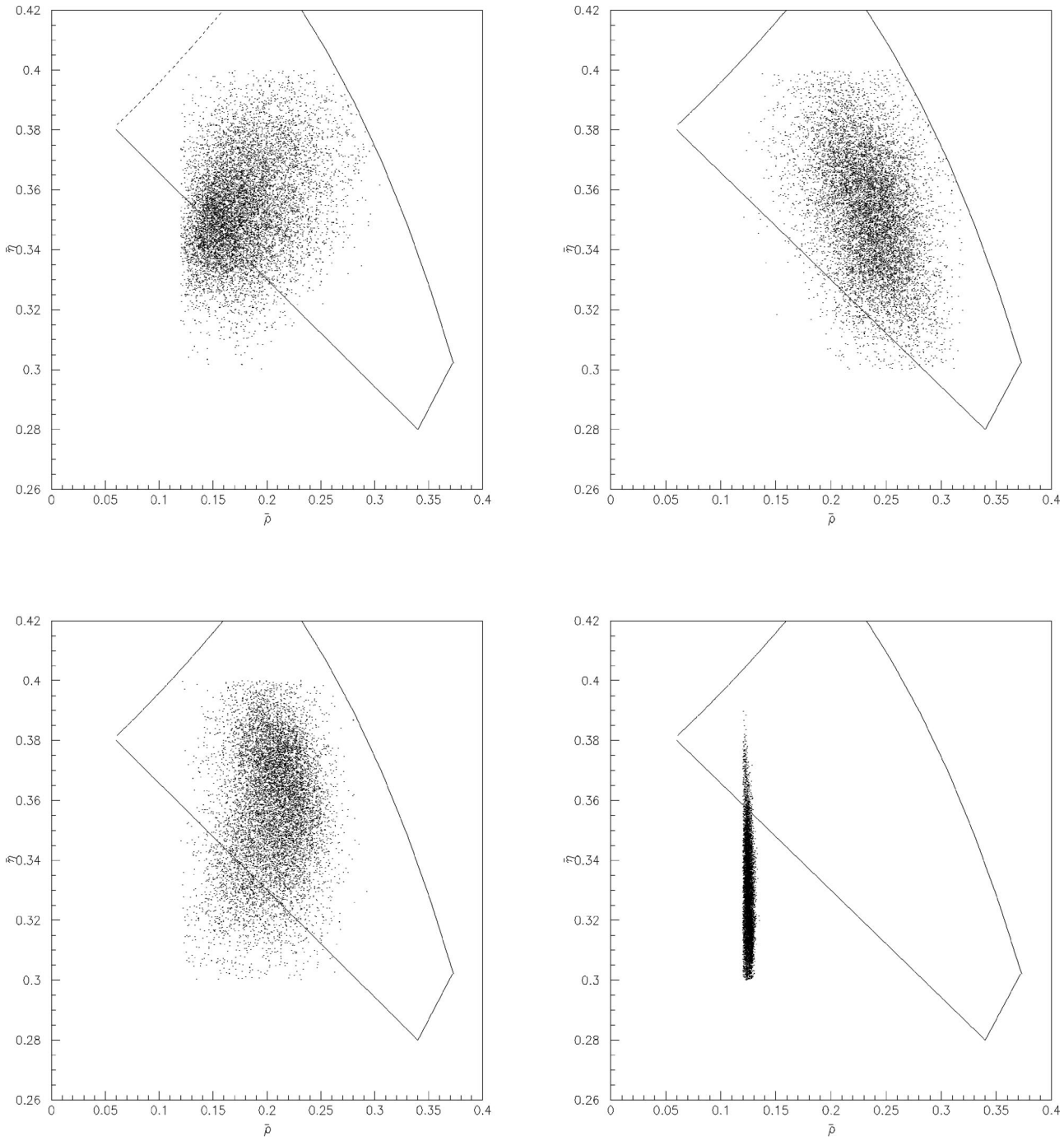

FIG. 9. Solutions for $\overline{\rho}$ and $\overline{\eta}$ of all four possible cases for the 24 parameter space (clockwise from top left): $(+\ +\ +)$, $(+\ +\ -)$, $(+\ -\ -)$, $(+\ -\ +)$. The delimited area is the allowed region in the $(\overline{\rho}, \overline{\eta})$ plane.

glets at the other orbifold fixed point $(+\ -\ -)$, the deviations from a pure democratic mass matrix are large for both mass matrices. Also in this case a small top mass seems to be favored (Fig. 4). The situation is different in the other two cases where the up- and down-type singlets are localized at different orbifold fixed points. In particular, the case with the doublets and down-type singlets right components localized at the zero fixed point and the up-type singlets at the other orbifold fixed point $(+\ -\ +)$ seems to be the one that allows a larger range for the top-quark mass values (Fig. 3). In this case the deviation from a pure democratic mass matrix for the up sector is bigger than the one for the down sector. As we will show in the next section this is also the only case for which we were able to find solutions for the 15 parameter version of the model. The fourth case, where the doublets and up-type singlets are at the same orbifold fixed point while the down-type singlets are at the other orbifold fixed point $(+\ +\ -)$, gives for the top-quark mass a very narrow value-region around 178 GeV (Fig. 2). In this case the mass matrix for the up sector is very close to a pure democratic

TABLE II. Parameter space values for the 4 different cases of the 24 parameter model and for the $(+\ -\ +)$ case of the 15 parameter model.

	$(24)^{(+++)}$	$(24)^{(++-)}$	$(24)^{(+-+)}$	$(24)^{(+--)}$	$(15)^{(+-+)}$
g_{Yu}	57.81	59.85	61.66	60.83	60.69
g_{Yd}	0.98	1.18	1.00	1.25	1.08
F_{q1}	1.389	0.482	3.152	2.233	1
F_{q2}	0.979	0.888	0.327	0.357	1
F_{q3}	0.787	2.522	0.485	1.069	1
F_{u1}	0.938	0.966	−0.112	−0.429	−1
F_{u2}	0.843	0.725	−0.629	−1.476	−1
F_{u3}	1.352	1.185	−0.516	−0.313	−1
F_{d1}	1.344	−1.024	1.062	−0.323	1
F_{d2}	1.013	−1.639	0.087	−0.847	1
F_{d3}	1.437	−0.014	1.244	−2.480	1
μ_{q1}	2.252	2.279	1.467	2.087	2.513
μ_{q2}	3.367	2.474	2.142	2.236	1.928
μ_{q3}	2.660	1.234	2.458	2.130	1.993
μ_{u1}	1.965	1.755	1.942	1.126	1.177
μ_{u2}	2.060	2.597	1.658	1.006	1.562
μ_{u3}	1.496	2.000	1.452	1.322	1.152
μ_{d1}	2.537	2.223	2.008	3.380	4.969
μ_{d2}	3.157	2.079	1.820	1.736	5.427
μ_{d3}	2.520	1.482	2.460	1.693	1.022
ϕ_{u1}	−0.0001	−0.0007	−0.0006	−0.0053	0.0153
ϕ_{u2}	0.0155	−0.0018	−0.0000	−0.0003	−0.0001
ϕ_{d1}	−0.0095	0.0122	0.0870	0.0218	−0.0423
ϕ_{d2}	−0.1607	−0.0951	−0.0035	−0.0525	−0.0279

mass matrix while the deviation from it is larger for the down sector. What is important to say here is that by looking at the four different cases, it seems that deviation from a DMM is bigger when left and right components are localized at different orbifold fixed points.

V. 15 PARAMETER VERSION

In this section we present the results for another particular choice of the model with 15 parameters, which correspond to all the Yukawa couplings with the same absolute value, $|F_{q,i}|=|F_{u,i}|=|F_{d,i}|=1$. The family symmetry and left-right symmetry are now broken only through the parameters μ's and phases θ's. The important point is that for the 15 parameter model choice we were able to find solutions only for the case corresponding to $f_q>0$, $f_u<0$, $f_d>0$ with the conditions that all μ's are bigger than one (6). In the other three cases we were not be able to find solutions if we decided to keep the constraints $\mu>1$. The fact that we found solutions only for one of the four possible cases does not obviously exclude completely the existence of solutions for the other three cases, but we believe that we can at least conclude that the configuration $f_q>0$, $f_u<0$, $f_d>0$ is favored with respect to the others.

In the following we give the numerical solutions for the model's parameters and physics quantities as in the cases of 24 parameter version (see also Table II).

(1) $F_{q,i}=1\ F_{u,i}=-1\ F_{d,i}=1$:

$$M_{u(15)}^{(+-+)}=60.69\ \text{GeV}\begin{pmatrix} 0.8968 & 0.8619e^{i0.153} & 0.8986 \\ 0.9520 & 0.9267 & 0.9532e^{-i0.0001} \\ 0.9469 & 0.9204 & 0.9481 \end{pmatrix}, \tag{55}$$

$$m_{u(15)}^{(+-+)}=0.0024\ \text{GeV},\quad m_{c(15)}^{(+-+)}=0.713\ \text{GeV},\quad m_{t(15)}^{(+-+)}=168.1\ \text{GeV}, \tag{56}$$

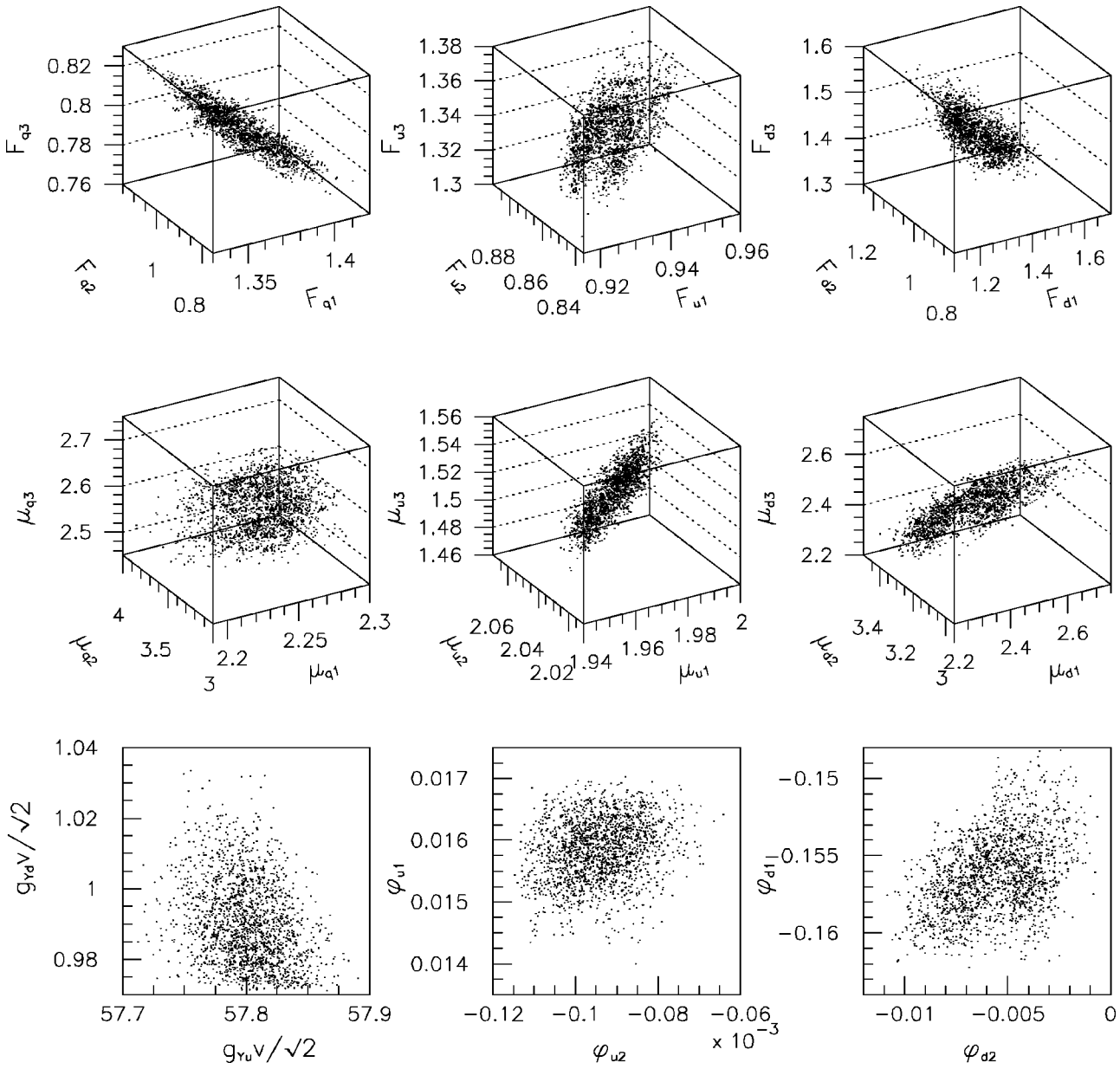

FIG. 10. Summary of the 24 parameter space corresponding to $f_{qi}>0\ f_{ui}>0\ f_{di}>0$.

$$M^{(+-+)}_{d(15)} = 1.08\ \text{GeV} \begin{pmatrix} 0.9086 & 0.8874e^{-i0.0423} & 0.9450 \\ 0.8414 & 0.8158 & 0.9829e^{-0.0279} \\ 0.8496 & 0.8245 & 0.9798 \end{pmatrix}, \tag{57}$$

$$m^{(+-+)}_{d(15)} = 0.0052\ \text{GeV}, \quad m^{(+-+)}_{s(15)} = 0.084\ \text{GeV}, \quad m^{(+-+)}_{b(15)} = 2.9\ \text{GeV}, \tag{58}$$

$$V^{(+-+)}_{\text{CKM}(15)} = \begin{pmatrix} 0.9696-0.0995i & 0.0917-0.2038i & 0.0024+0.0025i \\ -0.1140-0.1919i & 0.9737-0.0098i & 0.0436-0.0055i \\ 0.0018+0.0116i & -0.0422-0.0044i & 0.9990+0.0033i \end{pmatrix}, \tag{59}$$

$$\overline{\rho}^{(+-+)}_{(15)} = 0.16, \quad \overline{\eta}^{(+-+)}_{(15)} = 0.30, \quad J^{(+-+)}_{CP(15)} = -2.9\times 10^{-5}. \tag{60}$$

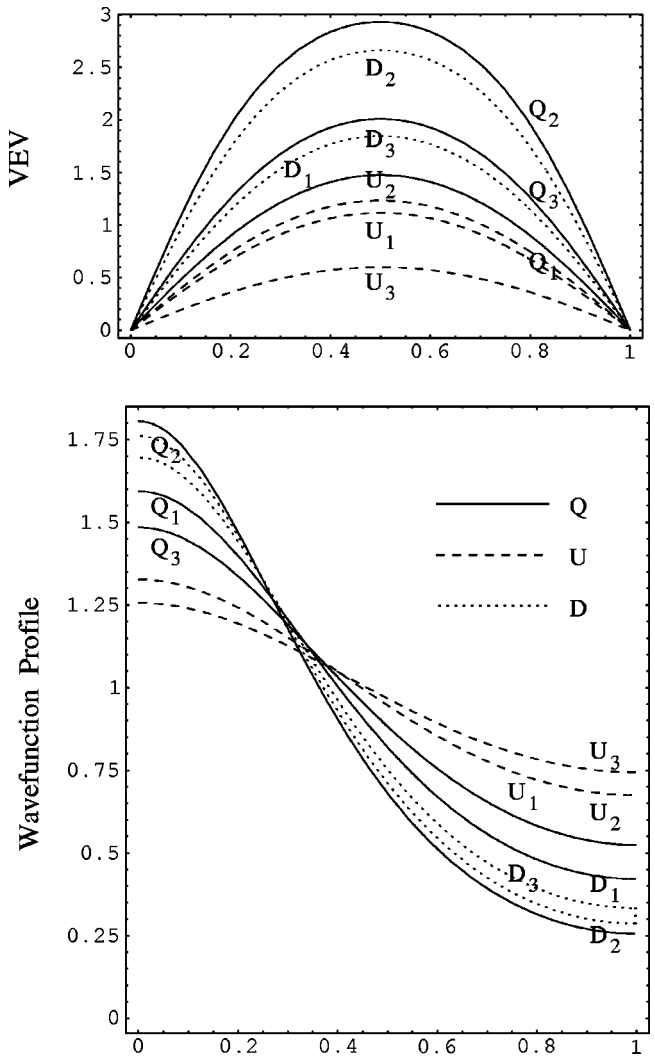

FIG. 11. Profile of the VEV's and of the wave functions for left and right components corresponding to $f_{qi}>0$, $f_{ui}>0$, $f_{di}>0$ for the 24 parameter space.

As it can be seen in the numerical example given above, also in the case of the 15 parameter version, as for all the 24 parameter cases, both mass matrices for the up and down sector are almost democratic. Our complete numerical survey also indicates that the 15 parameter case favors a small top mass, in contrast to the corresponding 24 parameter case $(+\ -\ +)$, which gives a much larger range for the top-quark mass.

VI. EPILOGUE

We suggest that using one extra dimension compactified on an S_1/Z_2 orbifold one is able to produce an almost democratic mass matrix and obtain the right mass spectrum and right CKM matrix. In the model presented the zero modes are localized only at the orbifold fixed points and different profiles for the zero mode wave functions are allowed. We show that in the case of the 24 parameter version of the model, for all four possible scenarios to localize the left- and right-handed components of quarks at one or the other orbifold fixed point, we were able to fit the mass spectrum and CKM matrix. On the other hand, in the case of the 15 parameter version of the model, which corresponds to having the universal absolute value of the Yukawa couplings with the background scalar field for the different fermion families, we were able to reproduce the right mass spectrum and right CKM only in the case with the doublets and down-type singlets localized at one orbifold fixed point and the up-type singlets at the other orbifold fixed point. Finally we just also explain how the existence of a sixth dimension could account for the different Yukawa couplings for the up and down sectors.

ACKNOWLEDGMENTS

We would like to thank Professor P.Q. Hung and Dr. M. Seco for valuable discussions, and the University of Virginia High Energy Theory Group for supporting our work.

[1] H. Georgi, A. K. Grant, and G. Hailu, Phys. Rev. D **63**, 064027 (2001).
[2] R. Jakiw and S. Rebbi, Phys. Rev. D **13**, 3398 (1976).
[3] N. Arkani-Hamed and M. Schmaltz, Phys. Rev. D **61**, 033005 (2000).
[4] A. Masiero, M. Peloso, L. Sorbo, and R. Tabbash, Phys. Rev. D **62**, 063515 (2000).
[5] D. E. Kaplan and T. M. Tait, J. High Energy Phys. **11**, 051 (2001).
[6] Y. Grossman and G. Perez, Phys. Rev. D **67**, 015011 (2001).
[7] P. Q. Hung and M. Seco, Nucl. Phys. **B653**, 123 (2003).
[8] P. Q. Hung, M. Seco, and A. Soddu, hep-ph/0311198 (2003); A. Soddu, Ph.D. thesis, University of Virginia (2003).
[9] E. A. Mirabelli and M. Schmaltz, Phys. Rev. D **61**, 113011 (2000).
[10] G. C. Branco, A. de Gouvea, and M. N. Rebelo, Phys. Lett. B **506**, 115 (2001).
[11] F. del Aguila and J. Santiago, J. High Energy Phys. **03**, 010 (2002).
[12] W.-F. Chang and J. N. Ng, J. High Energy Phys. **12**, 077 (2002).
[13] T. Teshima and T. Sakai, Prog. Theor. Phys. **97**, 653 (1997).
[14] A. Muck, A. Pilaftsis, and R. Ruckl, Phys. Rev. D **65**, 085037 (2002).
[15] S. Kirkpatrick, C. D. Gelatt, and M. P. Vecchi, Science **220**, 671 (1983).
[16] S. Kirkpatrick, J. Stat. Phys. **34**, 975 (1984).
[17] N. Metropolis, A. Rosenbluth, M. Rosenbluth, A. Teller, and E. Teller, J. Chem. Phys. **21**, 1087 (1953).
[18] W. H. Press, S. A. Teukolosky, W. T. Vetterling, and B. P. Flannery, *Numerical Recipes in C*, 2nd ed. (Cambridge, University Press, New York, 1992).